

# Vapor Phase near Infrared Spectroscopy of the Hydrogen Bonded Methanol–Trimethylamine Complex

Daryl L. Howard and Henrik G. Kjaergaard\*

Department of Chemistry, University of Otago, P.O. Box 56, Dunedin 9001, New Zealand

Received: March 13, 2006; In Final Form: May 25, 2006

The spectroscopy of the vapor phase hydrogen bonded complex formed between methanol and trimethylamine has been studied in the near-infrared region. A combination band involving one quantum of OH stretch and one quantum of COH bend has been observed for the complex. The much less intense first OH-stretching overtone transition has been tentatively assigned. This assignment is supported by anharmonic oscillator local mode calculations.

## Introduction

Hydrogen bonded complexes in the Earth's atmosphere have been shown to be of potential importance to climate change.<sup>1,2</sup> These complexes are generally held together by a weak hydrogen bond and are difficult to study under conditions relevant to the atmosphere. The water dimer is perhaps the only example that has been observed in the atmosphere,<sup>3</sup> and in the laboratory under atmospheric conditions.<sup>4</sup> One of the key questions regarding hydrogen bonded complexes is how their spectroscopy affects the absorption of solar radiation in the near-infrared (NIR) and visible wavelength regions. Simulations of the total absorption of solar radiation by atmospheric water dimer show it to be very sensitive to the bandwidth and shape of the dimer transitions.<sup>5</sup> This bandwidth and shape is not known due to the lack of experimental spectra.

Many species that undergo hydrogen bonding have relatively low vapor pressures and the equilibrium constants for the hydrogen bonded complexes in the vapor phase are typically small. The vibrational transitions affected by hydrogen bonding in a complex may be masked by overlap with the monomer transitions and overtone transitions are in general weaker than fundamental transitions. For these reasons, studies of hydrogen bonded systems in the vapor phase are mostly limited to fundamental transitions in the infrared (IR).<sup>6</sup>

To obtain experimental evidence for NIR transitions in complexes, we have chosen to investigate the NIR spectroscopy of the complex formed between methanol (MeOH) and trimethylamine (TMA). Although this complex is not present in any appreciable amount in the atmosphere, it is a favorable system for laboratory study. Both MeOH and TMA have relatively high vapor pressures to permit vapor phase study, and the binding energy of the complex formed is large enough for it to be present in equilibrium at room temperature.<sup>7–10</sup> Millen and Zabicky performed one of the first spectroscopic studies of hydrogen bonding in the vapor phase involving MeOH and TMA in the IR region between 3100 and 3600  $\text{cm}^{-1}$ .<sup>7</sup> They observed that, upon complexation to TMA, the OH-stretching frequency of MeOH was red shifted by 330  $\text{cm}^{-1}$ . Two weaker bands at approximately  $3350 \pm 145 \text{ cm}^{-1}$  were observed on either side of the OH-stretching band. These two bands were

attributed to sum and difference bands of the OH-stretching vibration with the low-frequency hydrogen bond vibration  $\nu_{\sigma}$ . In the far-IR spectrum of the MeOH–TMA complex, a band was observed at 142  $\text{cm}^{-1}$ , which was not found in the spectra of the individual components.<sup>11</sup> This band was assigned as the hydrogen bond vibration  $\nu_{\sigma}$ . The band was also observed in a subsequent far-IR study; however, the same result was also observed in mixtures of MeOH with either nitrogen or argon.<sup>12</sup> The intensity of the band also increased with increasing nitrogen or argon partial pressure, which led it to be named a “pressure enhanced methanol band.”<sup>12</sup> Thus the assignment of  $\nu_{\sigma}$  at 142  $\text{cm}^{-1}$  is not settled.

The MeOH–TMA system was determined to be a 1:1 complex from the pressure dependence of the associated OH-stretching band intensity;<sup>7</sup> i.e., the absorbance of the OH-stretching band of the complex is proportional to the product of the pressures of MeOH and TMA.

In addition, a few other studies of the MeOH–TMA complex have been performed. Proton nuclear magnetic resonance spectroscopy was used to monitor the temperature and pressure effects on the MeOH–TMA system to obtain the enthalpy and entropy.<sup>10</sup> Thermodynamic parameters were determined from pressure, volume and temperature studies<sup>8,9</sup> and from infrared relative intensity measurements.<sup>9</sup> A theoretical calculation on the MeOH–TMA system was performed at the B3LYP/6-31G-(d,p) level.<sup>13</sup> The only results reported from this calculation were the frequency changes in the  $\text{NC}_3$  bending modes of TMA upon complexation with MeOH.

## Experiment

Liquid MeOH (Aldrich, 99.9%) was dried with molecular sieves and degassed with the freeze–pump–thaw method on a vacuum line; otherwise, no further purification was performed. Anhydrous TMA (Matheson, 99%) was used without any further purification.

We have recorded the IR spectra of vapor phase MeOH, TMA and a mixture of the two to verify previous results.<sup>7,9</sup> The spectra were recorded at 1  $\text{cm}^{-1}$  resolution with a Bruker Equinox 55 FTIR spectrometer. A 10 cm path length gas cell equipped with KBr windows was used. MeOH and TMA were each recorded with a pressure of 50 Torr. For the mixture, 50 Torr MeOH was admitted to the vacuum line and followed by TMA until

\* To whom correspondence should be addressed. E-mail: henrik@alkali.otago.ac.nz. Fax: 64-3-479-7906. Phone: 64-3-479-5378.

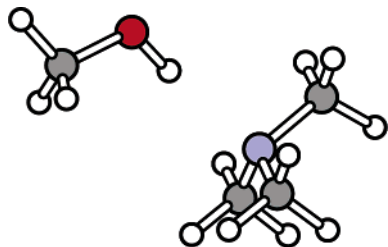


**Figure 1.** Geometry optimized structure of the MeOH–TMA complex.

the total pressure was 100 Torr. The infrared spectra were recorded at 19 °C.

The NIR spectra of MeOH and TMA were recorded with a Varian Cary 500 spectrophotometer. A 4.8 m path length gas cell (Infrared Analysis, Inc.) fitted with Infrasil quartz windows was used. The spectra of MeOH and TMA were each recorded with various pressures. To record the spectrum of the mixture, a certain pressure of MeOH was admitted first into the evacuated gas cell, followed by TMA, which was released in “bursts” to allow for good mixing. For example, an experiment was performed with 64 Torr MeOH and 502 Torr TMA for the individual component spectra, and 569 Torr total pressure for the mixture (of which MeOH composed of 64 Torr). Background scans with an evacuated cell were subtracted from the sample spectra. A 0.2 OD (optical density) neutral density filter was used as an attenuator in the reference beam path of the Cary 500.

### Computational Method

We have used an anharmonic oscillator local mode model to describe the OH-stretching mode in MeOH and the MeOH–TMA complex.<sup>14</sup> The details of this model is given in a recent paper.<sup>15</sup> The vibrational Hamiltonian is approximated by a Morse oscillator, which has the well-known energy expression

$$\tilde{\nu}/\nu = \tilde{\omega} - (\nu + 1)\tilde{\omega}x \quad (1)$$

where  $\tilde{\nu}$  is the transition energy in  $\text{cm}^{-1}$  from  $\nu = 0$  to  $\nu$ . The dipole moment function is approximated as a series expansion in the internal displacement coordinate  $q$ . The local mode frequency and anharmonicity and the dipole moment series expansion coefficients are determined from ab initio calculated potential energy and dipole moment curves. The grid points in the curves are calculated by serially displacing  $q$  by  $\pm 0.2$  Å from equilibrium in steps of 0.05 Å for a total of nine points. We have limited the series expansion of the dipole moment to fifth order.<sup>16,17</sup> The OH-stretching frequency and anharmonicity are obtained from the second-, third- and fourth-order derivatives of the potential energy with respect to the OH-stretching coordinate according to the equations given previously.<sup>15</sup> These derivatives are determined by fitting an eighth-order polynomial to the nine-point grid. Intensities are expressed in the dimensionless oscillator strength  $f$ .

The optimized MeOH, TMA and MeOH–TMA molecular geometries and the grid points were obtained with the QCISD/6-311++G(d,p) method. We have calculated the harmonic frequencies with the QCISD/6-31+G(d) method. The ab initio calculations were performed with MOLPRO.<sup>18</sup>

### Results and Discussion

The geometry optimized structure of the MeOH–TMA complex is shown in Figure 1. The complex has  $C_s$  symmetry, and the MeOH and TMA monomers respectively have  $C_s$  and  $C_{3v}$  symmetry. The complete structure of the complex is given

**TABLE 1: Calculated and Observed OH-Stretching Local Mode Parameters ( $\text{cm}^{-1}$ ) of MeOH and of the MeOH–TMA Complex**

	MeOH		MeOH–TMA	
	$\tilde{\omega}$	$\tilde{\omega}x$	$\tilde{\omega}$	$\tilde{\omega}x$
calculated <sup>a</sup>	3920.0	87.39	3629.6	121.1
scaled <sup>b</sup>	3855.7	86.14	3570.1	119.4
observed <sup>c</sup>	$3855.7 \pm 1.6$	$86.14 \pm 0.29$	3624	133

<sup>a</sup> Unscaled parameters calculated at the QCISD/6-311++G(d,p) level. <sup>b</sup> Calculated values scaled with the scaling factors  $\tilde{\omega} = 0.98360$  and  $\tilde{\omega}x = 0.9857$ . <sup>c</sup> From a fit of the observed  $\Delta\nu_{\text{OH}} = 1-4, 6, 7$  transitions.<sup>20</sup> Uncertainties are one standard deviation.

**TABLE 2: Calculated OH-Stretching Wavenumbers and Intensities of MeOH and of the MeOH–TMA Complex<sup>a</sup>**

$\Delta\nu_{\text{OH}}$	$\tilde{\nu}_f$	$\tilde{\nu}_b$	$\Delta\tilde{\nu}$	$f_f$	$f_b$	$f_b/f_f$
1	3683	3331	352	$2.8 \times 10^{-6}$	$1.9 \times 10^{-4}$	68
2	7195	6425	770	$7.0 \times 10^{-7}$	$2.0 \times 10^{-8}$	0.029
3	10534	9280	1254	$3.3 \times 10^{-8}$	$4.2 \times 10^{-9}$	0.13
4	13703	11898	1805	$1.4 \times 10^{-9}$	$6.6 \times 10^{-10}$	0.47

<sup>a</sup> Calculated with the scaled QCISD/6-311++G(d,p) local mode parameters from Table 1. The subscripts f and b refer to the OH bond in MeOH and MeOH–TMA, respectively.

as Supporting Information. The OH...N angle, or hydrogen bond angle ( $\angle\text{HB}$ ), is calculated to be nearly linear at approximately 179°, which is an optimal orientation for an intermolecular hydrogen bond.<sup>19</sup> The OH bond length of MeOH is calculated to lengthen substantially by approximately 0.013 Å upon complexation with TMA suggesting a strong hydrogen bond. The QCISD/6-311++G(d,p) calculated binding energy of the complex is 35  $\text{kJ mol}^{-1}$ .

In Table 1 we present the calculated OH-stretching local mode parameters of MeOH and MeOH–TMA obtained at the QCISD/6-311++G(d,p) level. The observed OH-stretching local mode parameters of MeOH, obtained from a fit of the observed  $\Delta\nu_{\text{OH}} = 1-4, 6,$  and  $7$  transitions<sup>20</sup> to eq 1, are also presented. The  $\Delta\nu_{\text{OH}} = 5$  transition was omitted from the fit due to a strong resonance. The calculated local mode frequency and anharmonicity of free MeOH are about 65 and 1  $\text{cm}^{-1}$  greater than the observed values, respectively. Vibrational harmonic frequencies calculated at the QCISD level are known to be high.<sup>17</sup> We have attempted to improve the accuracy by scaling the calculated local mode parameters. The ratio of the observed to calculated methanol local mode parameters in Table 1 were used to obtain the scaling factors, which are given in the footnote to Table 1 and applied to the OH-stretching local mode parameters of the complex. When MeOH is hydrogen bonded with TMA,  $\tilde{\omega}$  is calculated to drop by approximately 300  $\text{cm}^{-1}$  and  $\tilde{\omega}x$  to increase more than 30  $\text{cm}^{-1}$ . An increase in anharmonicity and decrease in frequency of the OH-stretching vibration is expected with hydrogen bonding.<sup>21</sup>

The calculated OH-stretching wavenumbers and intensities of free MeOH and MeOH–TMA are presented in Table 2, where the subscripts f and b refer to the free MeOH and hydrogen bonded MeOH OH-stretching bonds, respectively. The experimental wavenumbers for the MeOH–TMA complex are compared with those of MeOH in Table 3. In the fundamental region, the calculated redshift  $\Delta\tilde{\nu}$  is predicted to be 352  $\text{cm}^{-1}$ , which is in good agreement with observation. Our spectrum in the fundamental IR region is shown as Supporting Information and is in reasonable agreement with previous spectra.<sup>7,9</sup> The  $\nu_{\text{OH}}$  intensity of the complex is calculated to be nearly 70 times stronger than that for free MeOH, as seen in Table 2. The intensity increase of  $\nu_{\text{OH}}$  is considered to be the criterion for

**TABLE 3: Observed Wavenumbers ( $\text{cm}^{-1}$ ) of the OH-Stretching Vibration ( $\nu_{\text{OH}}$ ), the In-Plane COH-Bending Vibration ( $\delta_{\text{OH}}$ ) and of the Combination Band ( $\nu_{\text{OH}} + \delta_{\text{OH}}$ ) of MeOH and of the MeOH–TMA Complex**

parameter	MeOH	MeOH–TMA	$\Delta\tilde{\nu}^a$
$\nu_{\text{OH}}$	3681	3358	323
$\delta_{\text{OH}}$	1336 <sup>b</sup>	1473 <sup>c</sup>	−137
$\nu_{\text{OH}} + \delta_{\text{OH}}$	5017	4831	186
$2\nu_{\text{OH}} - \nu_{\sigma}$		6320 <sup>d</sup>	
$2\nu_{\text{OH}}$	7196	6450	746

<sup>a</sup> A negative sign denotes a blue shift. <sup>b</sup> From ref 32. <sup>c</sup> Not observed, but taken as  $(\nu_{\text{OH}} + \delta_{\text{OH}}) - \nu_{\text{OH}}$ . <sup>d</sup> Tentative.

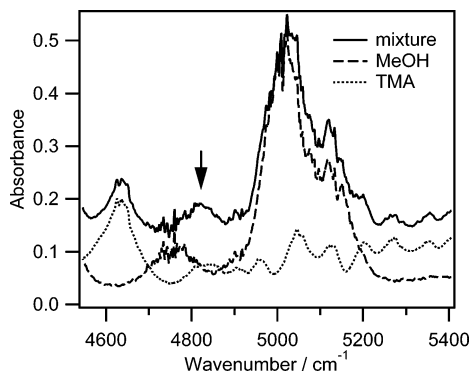


**Figure 2.** Spectra of 80 Torr MeOH, 80 Torr TMA, and a 161 Torr mixture of the two components recorded in a 4.8 m path length cell at 21 °C. The arrow points to the  $\nu_{\text{OH}} + \delta_{\text{OH}}$  transition of the complex.

hydrogen bonding.<sup>22</sup> The fundamental OH-stretching vibration of the MeOH–TMA complex is easily observed for two reasons. The first is that neither MeOH nor TMA absorb strongly in that wavenumber region; thus it is not masked by the monomer transitions. The second is that the intensity of the transition is very strong. The intensity increase compensates for the fact that only ~1–3% of TMA is complexed with MeOH at room temperature.<sup>9,23</sup>

The gas-phase NIR spectra of MeOH, TMA and the mixture of the two components are shown in Figure 2. The prominent absorption at 5017  $\text{cm}^{-1}$  is a methanol combination band,  $\nu_{\text{OH}} + \delta_{\text{OH}}$ , corresponding to a transition in which the OH-stretching and the predominantly in-plane COH-bending modes are each excited by one quantum of vibration. A new absorption feature is observed in the spectrum of the mixture that is not observed in the spectra of the individual components, and it is indicated with an arrow in Figure 2. It is assigned as the  $\nu_{\text{OH}} + \delta_{\text{OH}}$  transition of the complex. The transition of the complex is red shifted relative to that of the methanol monomer. The peak position and line shape of the complex transition was determined by spectral subtraction of the MeOH and TMA spectra from the spectrum of the mixture. The resultant absorption band of the spectral subtraction is shown in Figure 3. It is a Lorentzian profile centered at 4831  $\text{cm}^{-1}$  with a full width at half-maximum of 71  $\text{cm}^{-1}$ . To check the reproducibility of the experiment, the spectra of the individual components and the mixture were recorded at different pressures. Also shown in Figure 3 is the resultant band obtained from spectral subtraction of 64 Torr MeOH and 502 Torr TMA from a 569 Torr mixture. The contours of the two bands shown in Figure 3 are similar. Within experimental error, the integrated area of the two bands is proportional to the product of the pressures of the two components, which indicates 1:1 complex formation.

The  $\delta_{\text{OH}}$  transition that we report at 1473  $\text{cm}^{-1}$  was not observed, due to the strong  $\delta_{\text{CH}_3}$  transitions of TMA overlapping this area. We determine its wavenumber from the difference

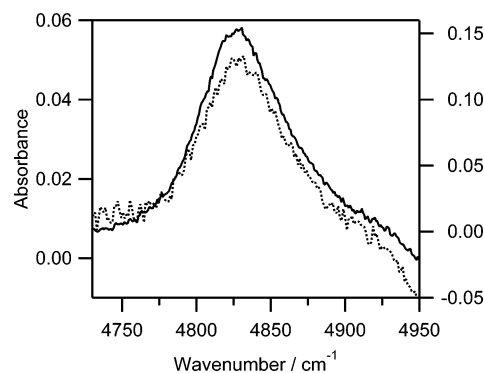


**Figure 3.**  $\nu_{\text{OH}} + \delta_{\text{OH}}$  band of the MeOH–TMA complex obtained by spectral subtraction of the individual components. The dotted line corresponds to the 161 Torr mixture (left ordinate). The solid line corresponds to the 569 Torr mixture.

between our observed  $\nu_{\text{OH}} + \delta_{\text{OH}}$  and  $\nu_{\text{OH}}$  transitions. This leads to a blue shift of 137  $\text{cm}^{-1}$  for  $\delta_{\text{OH}}$  upon hydrogen bonding. The blue shift of  $\delta_{\text{OH}}$  is expected upon hydrogen bonding.<sup>24,25</sup> The  $\delta_{\text{OH}}$  mode is not a local mode like the  $\nu_{\text{OH}}$  mode. Recent calculations have shown  $\delta_{\text{OH}}$  ( $\nu_6$ ) of MeOH consists of about two-thirds COH bend and one-third CH rock.<sup>26</sup> Our harmonic frequency calculation is in agreement with this. Additionally,  $\delta_{\text{OH}}$  is considered to be strongly mixed with the methyl rock-torsional combination band  $\nu_7 + \nu_{12}$ .<sup>27,28</sup> Our predicted 137  $\text{cm}^{-1}$  blue shift of  $\delta_{\text{OH}}$  upon hydrogen bonding will bring it into close resonance with the  $\nu_5$  HCH bend of MeOH and could also indicate that it no longer involves significant rocking motion. Thus the nature of the  $\delta_{\text{OH}}$  vibrational motion in the complex could be significantly different from that in free MeOH. Investigation of the normal modes from the harmonic frequency calculation of the complex indicate that  $\delta_{\text{OH}}$  is a mix of COH bend and HCH bend.

In the first OH-stretching overtone region, the value of  $\Delta\tilde{\nu}$  is predicted to be 770  $\text{cm}^{-1}$ . The intensity of the OH-stretching overtone of the complex is calculated to be about 30 times weaker than that for free MeOH. The “disappearance” of intensity in the first overtone of a relatively strongly hydrogen bonded system is known.<sup>19,29</sup> It can be explained by a cancellation of the contribution to the intensity of the different terms in the dipole moment expansion.<sup>30</sup>

Our calculated value for the  $2\nu_{\text{OH}}$  transition of the complex is 6425  $\text{cm}^{-1}$ . Sandorfy<sup>6</sup> has cited the unpublished work of Bernstein et al. in which the  $2\nu_{\text{OH}}$  transition of the complex was observed at 6292  $\text{cm}^{-1}$ . Initially, we were unable to locate a transition in this general region that could be assigned to the complex when we used the same experimental conditions as for the spectra shown in Figure 2. However, the use of greater TMA pressures will force more complex formation. The spectra of 66 Torr MeOH, 403 Torr TMA and of a 469 Torr mixture of the two components is shown in Figure 4 as an example. It is apparent from the spectra that any possible absorption due to the complex is very weak. After spectral subtraction, a very weak absorbance was found in the 6250–6500  $\text{cm}^{-1}$  region. The difference spectra are shown in Figure 5 for two different experimental conditions. The difference spectra were not entirely reproducible, but a common feature of two bands is observed. One weaker band located at 6320  $\text{cm}^{-1}$  is close to the 6292  $\text{cm}^{-1}$  value of Bernstein et al., and the other band at 6450  $\text{cm}^{-1}$  is in agreement with our calculated value of 6425  $\text{cm}^{-1}$ . The two bands were best fit by Gaussians and have line widths of ~62 and ~87  $\text{cm}^{-1}$ , respectively. It is puzzling that the band at 6450  $\text{cm}^{-1}$  was not noted by Bernstein et al., as we find it is slightly more intense.

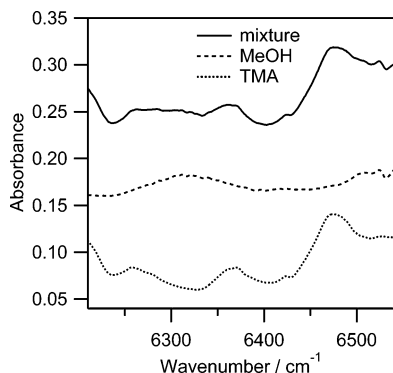


**Figure 4.**  $2\nu_{\text{OH}}$  region of the MeOH–TMA complex. Spectra of 66 Torr MeOH, 403 Torr TMA and a 469 Torr mixture of the two components. The spectra were recorded at 21 °C.

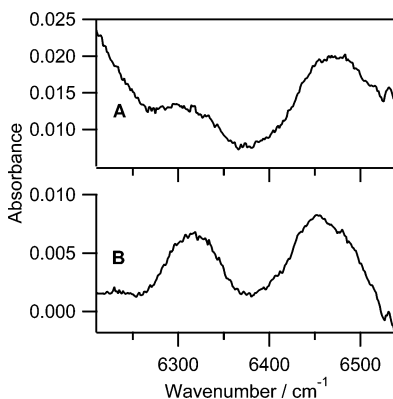


**Figure 5.**  $2\nu_{\text{OH}}$  region of the MeOH–TMA complex. (A) Residual spectrum of 51 Torr MeOH and 490 Torr TMA spectrally subtracted from a 549 Torr mixture of the two components (18 °C). (B) Residual spectrum of 66 Torr MeOH and 403 Torr TMA spectrally subtracted from a 469 Torr mixture of the two components (21 °C).

The local mode parameters obtained from the fit of our observed  $\nu_{\text{OH}}$  (3358  $\text{cm}^{-1}$ ) and  $2\nu_{\text{OH}}$  (6450  $\text{cm}^{-1}$ ) transitions of the complex to eq 1 yield  $\tilde{\omega} = 3624 \text{ cm}^{-1}$  and  $\tilde{\omega}_x = 133 \text{ cm}^{-1}$ , which are in reasonable agreement with our calculated values (Table 1). If we instead use the Bernstein et al. value for  $2\nu_{\text{OH}}$ , we obtain  $\tilde{\omega} = 3782 \text{ cm}^{-1}$  and  $\tilde{\omega}_x = 212 \text{ cm}^{-1}$ , which do not seem like reasonable local mode parameters. This anharmonicity is nearly a factor of 2.5 greater than that of free MeOH and is unreasonably high. Local mode parameters obtained from a fit of only two transitions, as done here, should be regarded as approximate.

Another interesting observation is that the two bands in the  $2\nu_{\text{OH}}$  region are approximately 130  $\text{cm}^{-1}$  apart. In the fundamental region, the separation between the weak sum and difference bands of the OH-stretching vibration with the low-frequency hydrogen bond vibration ( $\nu_{\text{OH}} \pm \nu_{\sigma}$ ) is  $\sim 140 \text{ cm}^{-1}$ . Thus it is possible we are observing the  $2\nu_{\text{OH}}$  transition of the complex coupling with the low-frequency hydrogen bond vibration  $\nu_{\sigma}$ ,  $2\nu_{\text{OH}} - \nu_{\sigma}$ . We have tentatively assigned this in Table 3. Our QCISD/6-31+G(d) calculation of the harmonic frequencies yields a hydrogen bond vibration at 180  $\text{cm}^{-1}$  in reasonable agreement with these observations. Although we did not observe a transition corresponding to  $2\nu_{\text{OH}} + \nu_{\sigma}$ , which would be expected around 6580  $\text{cm}^{-1}$ , it is possible the shoulder of the  $2\nu_{\text{OH}}$  band may have a contribution from the combination transition.

Absorption bands due to the MeOH dimer or larger MeOH complexes under various MeOH pressures from 10 to 80 Torr were only observed in the fundamental region. Several attempts were made to observe transitions due to hydrogen bonding in

the higher OH-stretching overtone regions with our photoacoustic spectrometer.<sup>15</sup> We were unable to observe any such transitions despite our calculations predicting higher relative intensity compared to MeOH than for the  $2\nu_{\text{OH}}$  region as seen in Table 2. This lack of observation could be due to a widening of the hydrogen bonded OH-stretching transition similar to what we have recently observed in the overtone spectra of a series of alkanediols.<sup>31</sup>

## Conclusion

The hydrogen bonded complex formed between methanol and trimethylamine was studied in the near-infrared region. The combination transition of the complex involving one quantum of OH stretch and one quantum of predominantly in-plane COH bend ( $\nu_{\text{OH}} + \delta_{\text{OH}}$ ) was observed for the first time. The transition is red shifted by 186  $\text{cm}^{-1}$  relative to the methanol monomer. The band contour of the transition is Lorentzian and has a full width at half-maximum of  $\sim 71 \text{ cm}^{-1}$ . The first OH-stretching overtone ( $2\nu_{\text{OH}}$ ) transition of the complex is tentatively assigned at 6450  $\text{cm}^{-1}$  and has a Gaussian line width of  $\sim 87 \text{ cm}^{-1}$ .

Anharmonic oscillator calculations were performed on free methanol and on the complex. The calculated OH-stretching transition wavenumbers for the complex are in good agreement with observation. Our calculations predict a 70-fold increase in the intensity of  $\nu_{\text{OH}}$  and a 30-fold drop in the intensity of  $2\nu_{\text{OH}}$  for the complex relative to free methanol. These changes in intensity partially account for the relative ease of observing the fundamental transition and the great difficulty observing the first overtone.

**Acknowledgment.** We thank the Marsden Fund administered by the Royal Society of New Zealand for support, the Lasers and Applications Research Theme at the University of Otago for use of their computer facilities, and the University of Otago Research Committee, by means of the University of Otago Postgraduate Publishing Award.

**Supporting Information Available:** Infrared spectra of MeOH, TMA and of their mixture in the 3100–3600  $\text{cm}^{-1}$  region. QCISD/6-311++G(d,p) optimized geometry of the MeOH–TMA complex in z-matrix form. This material is available free of charge via the Internet at <http://pubs.acs.org>.

## References and Notes

- Vaida, V.; Kjaergaard, H. G.; Feierabend, K. J. *Int. Rev. Phys. Chem.* **2003**, *22*, 203–219.
- Vigasin, A. A. *Molecular Complexes in Earth's, Planetary, Cometary, and Interstellar Atmospheres*; World Scientific: River Edge, NJ, 1998.
- Pfeilsticker, K.; Lotter, A.; Peters, C.; Bösch, H. *Science* **2003**, *300*, 2078–2080.
- Ptashnik, I. V.; Smith, K. M.; Shine, K. P.; Newnham, D. A. *Q. J. R. Meteorol. Soc.* **2004**, *130*, 2391–2408.
- Vaida, V.; Daniel, J. S.; Kjaergaard, H. G.; Goss, L. M.; Tuck, A. F. *Q. J. R. Meteorol. Soc.* **2001**, *127*, 1627–1643.
- Sandorfy, C. *Top. Curr. Chem.* **1984**, *120*, 41–84.
- Millen, D. J.; Zabicky, J. *Nature* **1962**, *196*, 889–890.
- Millen, D. J.; Mines, G. W. *J. Chem. Soc., Faraday Trans. 2* **1974**, *70*, 693–699.
- Fild, M.; Swiniarski, M. F.; Holmes, R. R. *Inorg. Chem.* **1970**, *9*, 839–843.
- Clague, A. D. H.; Govil, G.; Bernstein, H. J. *Can. J. Chem.* **1969**, *47*, 625–629.
- Ginn, S. G. W.; Wood, J. L. *Nature* **1963**, *200*, 467–468.
- Carlson, G. L.; Witkowski, R. E.; Fately, W. G. *Nature* **1966**, *211*, 1289–1291.
- Schreiber, V. M.; Rospenk, M.; Sobczyk, L. *Chem. Phys. Lett.* **1999**, *304*, 73–78.
- Kjaergaard, H. G.; Turnbull, D. M.; Henry, B. R. *J. Chem. Phys.* **1993**, *99*, 9438–9452.

- (15) Howard, D. L.; Jørgensen, P.; Kjaergaard, H. G. *J. Am. Chem. Soc.* **2005**, *127*, 17096–17103.
- (16) Howard, D. L.; Kjaergaard, H. G. *J. Chem. Phys.* **2004**, *121*, 136–140.
- (17) Low, G. R.; Kjaergaard, H. G. *J. Chem. Phys.* **1999**, *110*, 9104–9115.
- (18) Werner, H.-J.; Knowles, P. J.; Lindh, R.; Schütz, M.; Celani, P.; Korona, T.; Manby, F. R.; Rauhut, G.; Amos, R. D.; Bernhardsson, A.; Berning, A.; Cooper, D. L.; Deegan, M. J. O.; Dobbyn, A. J.; Eckert, F.; Hampel, C.; Hetzer, G.; Lloyd, A. W.; McNicholas, S. J.; Meyer, W.; Mura, M. E.; Nicklass, A.; Palmieri, P.; Pitzer, R.; Schumann, U.; Stoll, H.; Stone, A. J.; Tarroni, R.; Thorsteinsson, T. Molpro, version 2002.6, a package of ab initio programs, 2003.
- (19) Pimentel, G. C.; McClellan, A. L. *The Hydrogen Bond*; W. H. Freeman: San Francisco, 1960.
- (20) Rueda, D.; Boyarkin, O. V.; Rizzo, T. R.; Chirokolava, A.; Perry, D. S. *J. Chem. Phys.* **2005**, *122*, 044314.
- (21) Schuster, P.; Zundel, G., Sandorfy, C., Eds. *The Hydrogen Bond II. Structure and Spectroscopy*; North-Holland: Amsterdam, 1976.
- (22) Iogansen, A. V. *Spectrochim. Acta Part A* **1999**, *55*, 1585–1612.
- (23) Millen, D. J.; Zabicky, J. *J. Chem. Soc.* **1965**, 3080–3085.
- (24) Stuart, A. V.; Sutherland, G. B. B. M. *J. Chem. Phys.* **1956**, *24*, 559–570.
- (25) Asselin, M.; Sandorfy, C. *Can. J. Chem.* **1971**, *49*, 1539–1544.
- (26) Castillo-Chará, J.; Sibert, E. L., III. *J. Chem. Phys.* **2003**, *119*, 11671–11681.
- (27) Lees, R. M.; Xu, L.-H.; Johns, J. W. C.; Lu, Z.-F.; Winnewisser, B. P.; Lock, M.; Sams, R. L. *J. Mol. Spectrosc.* **2004**, *228*, 528–543.
- (28) Sibert, E. L., III; Castillo-Chará, J. *J. Chem. Phys.* **2005**, *122*, 194306.
- (29) Hilbert, G. E.; Wulf, O. R.; Hendricks, S. B.; Liddel, U. *J. Am. Chem. Soc.* **1936**, *58*, 548–555.
- (30) Kjaergaard, H. G.; Low, G. R.; Robinson, T. W.; Howard, D. L. *J. Phys. Chem. A* **2002**, *106*, 8955–8962.
- (31) Howard, D. L. Ph.D. Thesis, University of Otago, 2006.
- (32) Serrallach, A.; Meyer, R.; Günthard, H. *J. Mol. Spectrosc.* **1974**, *52*, 94–129.